

A Local Spin Model To Describe the Magnetic Interactions in Biological Molecules Containing [4Fe–4S]⁺ Clusters. Application to Ni–Fe Hydrogenases[†]

Patrick Bertrand,* Philippe Camensuli, Claude More, and Bruno Guigliarelli

Contribution from the Laboratoire de Bioénergétique et Ingénierie des Protéines, UPR 9036 CNRS, Université de Provence, Centre St. Jérôme C241 13397 Marseille Cedex 20, France

Received June 19, 1995[⊗]

Abstract: Structural information on the relative arrangement of paramagnetic centers can be obtained through the quantitative study of their magnetic interactions based on the numerical simulation of EPR spectra recorded at different microwave frequencies. In a recent work, we have shown that such studies must explicitly take into account the delocalization of the magnetic moments over polynuclear clusters, and we have presented a local spin model suited for valence-localized clusters (Bertrand, P.; More, C.; Guigliarelli, B.; Fournel, A.; Bennet, B.; Howes, B. *J. Am. Chem. Soc.* **1994**, *116*, 3078–3086). In this paper, we examine the more general situation in which the cluster contains partially or completely delocalized mixed-valence pairs. This situation is encountered in particular in the case of [4Fe–4S] clusters which are ubiquitous in biological systems. A model is presented and developed for a system containing a [4Fe–4S]⁺ cluster magnetically coupled to a mononuclear center. This model is then applied to the study of the magnetic interactions between the nickel center and the proximal [4Fe–4S]⁺ cluster in the active form of *Desulfovibrio gigas* hydrogenase. The arrangement at atomic resolution deduced from this study is compared to that given by a recent X-ray crystal study carried out on the inactive form of the same enzyme (Volbeda, A.; Charon, M. H.; Piras, C.; Hatchikian, E. C.; Frey, M.; Fontecilla-Camps, J. C. *Nature* **1995**, *373*, 580–587).

Introduction

The quantitative study of the magnetic interactions between paramagnetic centers, based on the numerical simulation of EPR spectra recorded at different microwave frequencies, has been used for a long time to obtain structural information in metalloproteins. These simulations generally rely on a point dipole model in which the delocalization of the magnetic moments over the paramagnetic centers is disregarded. We have shown recently that, in the case of polynuclear centers, the distances and the exchange parameters given by such a model are necessarily *effective parameters* whose values are dependent not only on the intercenter interactions but also on the electronic structure of the centers.¹ In order to take into account the delocalization of the magnetic moments, it is necessary to use a *local spin* description in which the magnetic interactions between all the paramagnetic sites of the system are explicitly considered.¹ In principle, such a description should be able to bring structural information “at atomic resolution” on the relative arrangement of the interacting centers. We have recently elaborated such a model for a system comprising a dinuclear cluster interacting with a mononuclear or a dinuclear center, and we used it to solve an old and controversial issue, concerning the relative arrangement of the molybdenum center and of one of the [2Fe–2S] center (center 1) in the enzyme xanthine oxidase.¹ Using the same model, we have shown that the lack of detectable magnetic interaction between a [2Fe–2S]⁺ center and a flavin semiquinone radical located 12 Å apart in phthalate dioxygenase reductase of *Pseudomonas cepacia* is due to a magic magnetic configuration in which the dipolar interactions cancel.² This enabled us to identify unambiguously the reducible iron site of the [2Fe–2S] cluster.²

The polynuclear centers most frequently found in metalloproteins are of the [4Fe–4S]^{1+/2+} type. They are ubiquitous as low potential redox centers in ferredoxins, in membrane bound complexes of the respiratory and photosynthetic electron transfer chains, and in a great variety of metalloenzymes. A growing body of data indicates that these centers can also possess a catalytic activity in some enzymes.³ It is often possible to prepare these systems in a redox state in which a [4Fe–4S]⁺ cluster interacts magnetically with other paramagnetic centers. Actually, 2x[4Fe–4S] ferredoxins have been considered for a long time as the paradigm of biological molecules giving an EPR spectrum displaying magnetic interaction effects.⁴ Thus, it appears very important to build a local spin model to describe the magnetic interactions in systems in which [4Fe–4S]⁺ centers are involved. Such a model cannot be a simple extension of that previously proposed for dinuclear clusters, because [4Fe–4S]⁺ clusters are valence-delocalized systems. This introduces a further complexity which must be properly treated in any realistic local spin description.

In this paper, we present a local spin model suited for systems containing a [4Fe–4S]⁺ cluster magnetically coupled to another paramagnetic species. For the sake of simplicity, this species is taken as a mononuclear center, but the extension to the case of a polynuclear center is obvious. The most general model contains a number of unknown parameters that cannot be determined experimentally, and a practical implementation based on reasonable simplifying assumptions is presented. This model is then applied to the study of the magnetic interactions between the nickel center and the iron–sulfur clusters in the active form of the Ni–Fe hydrogenase of *Desulfovibrio gigas*. By using the point dipole approximation, we have shown recently that

[†] Keywords: magnetic interactions, EPR, iron–sulfur clusters, metalloprotein, Ni–Fe hydrogenase.

[⊗] Abstract published in *Advance ACS Abstracts*, February 1, 1996.

(1) Bertrand, P.; More, C.; Guigliarelli, B.; Fournel, A.; Bennet, B.; Howes, B. *J. Am. Chem. Soc.* **1994**, *116*, 3078–3086.

(2) Bertrand, P.; More, C.; Camensuli, P. *J. Am. Chem. Soc.* **1995**, *117*, 1807–1809.

(3) Cammack, R. *Adv. Inorg. Chem.* **1992**, *38*, 281–322.

(4) Mathews, R.; Charlton, S.; Sands, R. H.; Palmer, G. *J. Biol. Chem.* **1974**, *249*, 4326–4328.

the static and dynamic effects of these interactions are well explained by the coupling of the nickel center to a single $[4\text{Fe}-4\text{S}]^+$ center.⁵ The intercenter distance given by this study is 8.6 Å, which is much shorter than the center-to-center distance of about 12 Å given by a recent X-ray crystal study carried out at 2.85 Å resolution on the inactive form of the enzyme.⁶ In the present work, we use the local spin model to compare accurately the relative arrangement of the metal centers in the two forms of the enzyme.

Materials and Methods

The experimental EPR spectra given by the Ni-Fe hydrogenase from *D. gigas* at X-band, Q-band, and S-band are those published in ref 5. Their numerical simulation was carried out by a new version of the program DIPLOC¹ adapted to the case of Hamiltonian 2. In this program, the spectral broadening is assumed to originate from strain effects which are described by a statistical distribution of the magnetic and structural parameters. The numerical simulations presented in this work were obtained by considering only *g*-strain effects. The distribution of the *g* tensor around a mean value \bar{g}_0 was described by a three-dimensional tensor \bar{p} whose principal elements are random variables p_i characterized by their standard deviations σ_i . In practice, good simulations were obtained by assuming that \bar{g}_0 and \bar{p} are collinear and by taking the random variables to be fully positively correlated. For the Ni center of *D. gigas* hydrogenase, these parameters have already been determined from a numerical simulation of the *unsplit* Ni-C spectrum.⁵

The determination of the numerous adjustable parameters involved in the local spin Hamiltonian was greatly facilitated by the results of a previous study which was based on the point dipole approximation⁵ and by resorting to a specially written regression program called REGRES. This program uses the following merit function

$$\chi^2 = \frac{\sum_i^N (y_i - y(x_i, p))^2}{\sum_i^N y_i^2}$$

where (x_i, y_i) are the coordinates of the *N* points obtained by digitization of the experimental spectrum and $y(x_i, p)$ the spectrum calculated with the set of parameters *p*. The adjustable parameters of the model were estimated by using the iterative Levenberg-Marquardt method.⁷

Magnetic Interactions between a $[4\text{Fe}-4\text{S}]^+$ Cluster and a Mononuclear Center

Consider a tetranuclear cluster whose metal sites labeled a, b, c, d interact magnetically with a mononuclear center m. When the valences of the metal ions are trapped, the local spin Hamiltonian describing the magnetic interactions is given by

$$H = H_Z + H_{\text{ex}} + H_{\text{dip}} \quad (1)$$

$$H_Z = -\bar{\mu}_m \cdot \bar{B} - \sum_{\alpha} \bar{\mu}_{\alpha} \cdot \bar{B}$$

$$H_{\text{ex}} = \sum_{\alpha} -2\bar{S}_{\alpha} \cdot \tilde{J}_{\alpha m} \cdot \bar{S}_m$$

$$H_{\text{dip}} = (\mu_0/4\pi) \sum_{\alpha} r_{\alpha m}^{-3} (\bar{\mu}_{\alpha} \cdot \bar{\mu}_m - 3(\bar{u}_{\alpha m} \cdot \bar{\mu}_{\alpha})(\bar{u}_{\alpha m} \cdot \bar{\mu}_m))$$

In these expressions, \bar{S}_{α} and $\bar{\mu}_{\alpha}$ represent the spin and the magnetic moment of site α , and $r_{\alpha m}$, $\bar{u}_{\alpha m}$ define the distance

(5) Guigliarelli, B.; More, C.; Fournel, A.; Asso, M.; Hatchikian, E. C.; Williams, R.; Cammack, R.; Bertrand, P. *Biochemistry* **1995**, *34*, 4781-4790.

(6) Volbeda, A.; Charon, M. H.; Piras, C.; Hatchikian, E. C.; Frey, M.; Fontecilla-Camps, J. C. *Nature* **1995**, *373*, 580-587.

and the direction between the mononuclear center and metal site α . This Hamiltonian, which is a simple extension of that presented in ref 1, is not appropriate for $[4\text{Fe}-4\text{S}]^+$ clusters. This is due to the fact that these clusters contain a delocalized mixed-valence (Fe(III), Fe(II)) pair according to low-temperature Mossbauer spectroscopy experiments,⁸⁻¹¹ so that, if we note a and b the two metal sites of this mixed-valence pair, the question that arises concerns which value must be taken for \bar{S}_a , \bar{S}_b and $\bar{\mu}_a$, $\bar{\mu}_b$. The aim of this section is to transform Hamiltonian 1 in order to adapt it to this situation. Our treatment follows closely those presented in refs 12-14.

Let $\psi_{S,M}$ be a function describing the state of the $[4\text{Fe}-4\text{S}]^+$ cluster, characterized by a value *S* of the total spin $S = \bar{S}_1 + \bar{S}_2 + \bar{S}_3 + \bar{S}_4$. The \bar{S}_i are the local spins involved in the spin coupling scheme with $\bar{S}_1 = \bar{S}_c$, $\bar{S}_2 = \bar{S}_d$, and $\bar{S}_1 = \bar{S}_2 = \bar{S}_4 = 2$, $\bar{S}_3 = 5/2$. We define two functions $\psi_{S,M}^a$, $\psi_{S,M}^b$ characterized by the same spin function as $\psi_{S,M}$ but describing two valence-trapped states in which the excess electron is localized on a and b, respectively. In state $\psi_{S,M}^a$ one has $S_a = S_4$, $S_b = S_3$, and the magnetic moments carried by the two sites are given by

$$\bar{\mu}_a = -\beta \bar{g}_4^a \cdot \bar{S}_4, \quad \bar{\mu}_b = -\beta \bar{g}_3^a \cdot \bar{S}_3$$

Similarly, in state $\psi_{S,M}^b$, $S_a = S_3$, $S_b = S_4$ and

$$\bar{\mu}_a = -\beta \bar{g}_3^b \cdot \bar{S}_3, \quad \bar{\mu}_b = -\beta \bar{g}_4^b \cdot \bar{S}_4$$

In these expressions, \bar{g}_i^{α} represents the *g* tensor of a given site when it carries the spin \bar{S}_i and when the excess electron is localized on site α . In the presence of valence delocalization, the states of the $[4\text{Fe}-4\text{S}]^+$ cluster can be written $\psi_{S,M} = c_a \psi_{S,M}^a + c_b \psi_{S,M}^b$ where c_a and c_b are mixing coefficients. It follows that, within the $\{|S, M\rangle | S_m, M_m\rangle\}$ subspace, the local spin Hamiltonian can be written

$$H_{\text{int}} = H_Z + H_{\text{ex}} + H_{\text{dip}} \quad (2)$$

$$H_Z = -\beta \bar{B} \cdot \bar{g}_m \cdot \bar{S}_m - \beta \bar{B} \cdot \bar{g} \cdot \bar{S}$$

$$H_{\text{ex}} = -2\bar{S} \cdot \tilde{J} \cdot \bar{S}_m$$

$$H_{\text{dip}} = (\mu_0/4\pi) \sum_{\alpha} r_{\alpha m}^{-3} (\bar{\mu}_{\alpha} \cdot \bar{\mu}_m - 3(\bar{u}_{\alpha m} \cdot \bar{\mu}_{\alpha})(\bar{u}_{\alpha m} \cdot \bar{\mu}_m))$$

with

$$\bar{g} = \sum_i K_i \bar{g}_i \quad (3)$$

$$\bar{g}_3 = |c_a|^2 \bar{g}_3^a + |c_b|^2 \bar{g}_3^b$$

$$\bar{g}_4 = |c_a|^2 \bar{g}_4^a + |c_b|^2 \bar{g}_4^b$$

$$\tilde{J} = K_1 \tilde{J}_{\text{cm}} + K_2 \tilde{J}_{\text{dm}} + K_3 [|c_a|^2 \tilde{J}_{\text{bm}}^a + |c_b|^2 \tilde{J}_{\text{am}}^b] + K_4 [|c_a|^2 \tilde{J}_{\text{am}}^a + |c_b|^2 \tilde{J}_{\text{bm}}^b] \quad (4)$$

(7) Press, W. H.; Flannery, B. P.; Teukolsky, S. A.; Vetterling, W. T. *Numerical Recipes*; Cambridge University Press: 1986; pp 498-546.

(8) Middleton, P.; Dickson, D. P. E.; Johnson, C. E.; Rush, J. D. *Eur. J. Biochem.* **1978**, *88*, 135-141.

(9) Carney, M. J.; Papaefthymiou, G. C.; Spartalian, K.; Frankel, R. B.; Holm, R. H. *J. Am. Chem. Soc.* **1988**, *110*, 6084-6095.

(10) Lindhahl, P. A.; Day, E. P.; Kent, T. A.; Orme-Johnson, W. H.; Münck, E. *J. Biol. Chem.* **1985**, *260*, 11160-11173.

(11) Auric, P.; Gaillard, J.; Meyer, J.; Moulis, J. M. *Biochem. J.* **1987**, *242*, 525-530.

$$\begin{aligned} \bar{\mu}_a &= -\beta[|c_a|^2 K_4 \tilde{g}_4^a + |c_b|^2 K_3 \tilde{g}_3^b] \bar{S}, & \bar{\mu}_b &= -\beta[|c_a|^2 K_3 \tilde{g}_3^a + \\ & |c_b|^2 K_4 \tilde{g}_4^b] \bar{S}, & \bar{\mu}_c &= -\beta K_1 \tilde{g}_1 \bar{S}, & \bar{\mu}_d &= -\beta K_2 \tilde{g}_2 \bar{S} \end{aligned} \quad (5)$$

These expressions are derived by assuming that the overlap of the orbitals centered on sites a and b between which the excess electron is exchanged is sufficiently small that cross terms between $\psi_{S,M}^a$ and $\psi_{S,M}^b$ can be neglected. The K_i are spin coupling coefficients resulting from the application of the Wigner-Eckart theorem, whose value depend on the spin coupling scheme leading to the $|S,M\rangle$ spin functions. For example, the ground state of $[4\text{Fe-4S}]^+$ clusters is generally characterized by $S = 1/2$, and a number of arguments indicate that this arises from the antiferromagnetic coupling of $S_{12} = 4$ with $S_{34} = 9/2$, where $\bar{S}_{12} = \bar{S}_1 + \bar{S}_2$ and $\bar{S}_{34} = \bar{S}_3 + \bar{S}_4$.^{12,13} In this case, the K_i are given by

$$K_1 = K_2 = -4/3 \quad K_3 = 55/27 \quad K_4 = 44/27 \quad (6)$$

This set of K_i will be used throughout this study.

The expression of the parameters appearing in Hamiltonian 2 deserves some comments. We first observe that, in the presence of valence delocalization, the g tensor of the $[4\text{Fe-4S}]^+$ cluster given by eq 3 depends *a priori* on four ferrous and two ferric local g tensors. This reduces to three ferrous and one ferric tensors either when one mixing coefficient is equal to 1 and the other to 0, that is to say when the valences are trapped, or when the a and b sites are equivalent: $\tilde{g}_3^a = \tilde{g}_3^b$ and $\tilde{g}_4^a = \tilde{g}_4^b$. In this last case, \tilde{g} no longer depends on the mixing coefficients. Owing to the low-lying excitations energies of the ferrous sites,^{15,16} the ferrous g tensors are expected to be very sensitive to variations of the structure and the environment of the $[4\text{Fe-4S}]^+$ cluster in the protein. This cause of variability, together with the large number of parameters determining the g tensor of $[4\text{Fe-4S}]^+$ clusters, may explain why the variations of their principal components from one protein to another do not appear to be correlated, contrary to what is observed for $[2\text{Fe-2S}]^+$ clusters.¹⁷ According to expression 4, the exchange parameter \tilde{J} is determined, on the one hand, by six terms like $\tilde{J}_{\alpha m}^\beta$ which measures the efficiency of the superexchange pathway between sites α and m when the excess electron is localized on β , and, on the other hand, by the mixing coefficients and the spin coupling coefficients which are imposed by the internal electronic structure of the $[4\text{Fe-4S}]^+$ cluster. Thus, the parameter \tilde{J} appearing in Hamiltonian 2 is an *effective* parameter whose magnitude and sign depend on a number of independent contributions. The dipolar term \mathcal{H}_{dip} of Hamiltonian 2 results from the interactions between the mononuclear center m and each metal site of the $[4\text{Fe-4S}]^+$ cluster. Equations 5 giving the expression of the magnetic moments $\bar{\mu}_a$ and $\bar{\mu}_b$ carried by the mixed-valence pair are new. These expressions involve four different local g tensors and simplify only when the valences are trapped.

Hamiltonian 2 is useful in the usual situation where the ground state of the $[4\text{Fe-4S}]^+$ cluster is well separated from the excited states and can be characterized by a value $S = S^0$ of

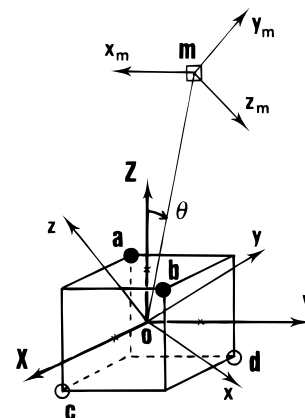


Figure 1. Structural model used to describe the magnetic interactions between a $[4\text{Fe-4S}]^+$ cluster and a mononuclear center m . The iron ions of the mixed-valence (Fe(III),Fe(II)) pair and the Fe(II) ions are represented by full circles and open circles, respectively. The inter-center vector $O\vec{m}$ is located by its polar coordinates (r, θ, φ) in the axes system (X, Y, Z) . The sets (x, y, z) and (x_m, y_m, z_m) represent the magnetic axes of the $[4\text{Fe-4S}]^+$ cluster and mononuclear center m , respectively.

the total spin. In this case, the energy levels and the eigenfunctions resulting from the magnetic interactions between the $[4\text{Fe-4S}]^+$ cluster and the mononuclear center are obtained by diagonalizing Hamiltonian 2 within the subspace $\{|S^0, M\rangle |S_m, M_m\rangle\}$. However, the unknown parameters appearing in this Hamiltonian are too numerous to be determined by a numerical simulation of experimental EPR spectra. In the following section, we examine how the different terms of this Hamiltonian can be treated in practical applications of the model.

Practical Implementation of the Model

We first consider the Zeeman term. The principal components of the $[4\text{Fe-4S}]^+$ g tensor can often be determined experimentally by simulating the frozen solution EPR spectrum of the system prepared in a redox state in which the cluster is magnetically isolated. However, in a local spin description, the orientation of the magnetic axes of the $[4\text{Fe-4S}]^+$ cluster with respect to the cubane structure must also be specified. As far as we know, no information on this point is available for $[4\text{Fe-4S}]^+$ centers in proteins. In the case of model complexes, single crystal EPR experiments have shown that the orientation of the magnetic axes may vary from one complex to the other.¹⁸⁻²⁰ For that reason, we have defined this orientation by a set of Euler angles $(\alpha', \beta', \gamma')$ which are considered as free parameters (Figure 1). In expression 4 giving the exchange parameter \tilde{J} , the different terms arise from weak long-range superexchange interactions. All the simulations presented in this paper were carried out by considering only the dominant isotropic component of these interactions. We now consider the dipolar terms and eq 5 giving the expression of the magnetic moments. Some pieces of information about the level of valence delocalization in the $S^0 = 1/2$ ground state of $[4\text{Fe-4S}]^+$ clusters in proteins comes from low temperature Mossbauer and ENDOR studies carried out on ^{57}Fe derivatives, which indicate that the hyperfine components of the two sites of the mixed-valence (Fe(III), Fe(II)) pair are essentially equal.⁸⁻¹⁰ The hyperfine tensors \tilde{A}_a and \tilde{A}_b probed by these techniques are related to the local

(12) Noodleman, L. *Inorg. Chem.* **1991**, *30*, 246-256.

(13) Noodleman, L. *Inorg. Chem.* **1991**, *30*, 256-264.

(14) Bertrand, P. *Inorg. Chem.* **1993**, *32*, 741-745.

(15) Noodleman, L.; Case, D. A. *Adv. Inorg. Chem.* **1992**, *38*, 423-470.

(16) Mousesca, J. M.; Chen, J. L.; Noodleman, L.; Bashford, D.; Case, D. A. *J. Am. Chem. Soc.* **1994**, *116*, 11898-11914.

(17) Bertrand, P.; Guigliarelli, B.; More, C. *New J. Chem.* **1991**, *15*, 445-454.

(18) Gloux, J.; Gloux, P.; Lamotte, B.; Rius, G. *Phys. Rev. Lett.* **1985**, *54*, 599-602.

(19) Gloux, J.; Gloux, P.; Hendriks, H.; Rius, G. *J. Am. Chem. Soc.* **1987**, *109*, 3220-3224.

(20) Gloux, J.; Gloux, P.; Lamotte, B.; Mousesca, J. M.; Rius, G. *J. Am. Chem. Soc.* **1994**, *116*, 1953-1961.

hyperfine tensors by equations similar to eqs 5¹⁴

$$\tilde{A}_a = |c_a|^2 K_4 \tilde{a}_4^a + |c_b|^2 K_3 \tilde{a}_3^b$$

$$\tilde{A}_b = |c_a|^2 K_3 \tilde{a}_3^a + |c_b|^2 K_4 \tilde{a}_4^b$$

Since the spin coupling coefficients K_3 and K_4 differ significantly in all spin coupling schemes proposed for the $S^0 = 1/2$ ground state, the Mossbauer and ENDOR data suggest that the two sites are equivalent

$$\tilde{a}_4^a = \tilde{a}_4^b = \tilde{a}_4, \quad \tilde{a}_3^a = \tilde{a}_3^b = \tilde{a}_3$$

and that the valence delocalization is complete

$$|c_a|^2 = |c_b|^2 = 1/2$$

Independent arguments based on theoretical energy level calculations favor a fully delocalized mixed-valence pair for the doublet ground states.^{12,13} In these conditions, the magnetic moments $\bar{\mu}_a$ and $\bar{\mu}_b$ given by eqs 5 can be written

$$\bar{\mu}_a = \bar{\mu}_b = -\beta/2[K_4 \tilde{g}_4 + K_3 \tilde{g}_3] \bar{S}$$

Even with this important simplification, we are left with one ferric and three ferrous local g tensors whose principal components and principal axes cannot be determined experimentally. However, the anisotropy of these tensors is expected to be moderate if one refers to the case of $[2\text{Fe}-2\text{S}]^+$ clusters in which it is less than 5%.¹⁷ For that reason, we have chosen to replace these local g tensors by scalars for the calculation of the dipolar terms. The ferric g value was taken equal to 2.025, the average of the ferric site components in $[2\text{Fe}-2\text{S}]^+$ clusters,¹⁷ and the three ferrous g values were taken equal to

$$g_1 = g_2 = g_4 = (g_{av} - K_3 g_3)/(1 - K_3) \quad (7)$$

where $g_{av} = (g_x + g_y + g_z)/3$ is the average of the three components of the $[4\text{Fe}-4\text{S}]^+$ g tensor. Equation 7 is the particular form taken by eq 3 when all g tensors are isotropic and all ferrous sites are equivalent. The error introduced by this procedure in the calculation of the dipolar terms is expected to be about a few percent, and the resulting error on the calculated EPR lines is probably even smaller due to cancellation effects. Actually, we have checked that the EPR spectra calculated in this way in the present study are essentially identical to those calculated by restoring their full anisotropy to the ferrous g tensors. This check was done by taking the axes of all local ferrous g tensors parallel.

The geometrical parameters describing the system are summarized in Figure 1. The location of the four iron ions of the $[4\text{Fe}-4\text{S}]^+$ cluster is defined by the set of axes (X, Y, Z) , Z being perpendicular to both the ab and cd directions. The Fe-Fe distance is taken equal to 2.7 Å. The intersite distances r_{am} and vectors \bar{u}_{am} needed for the calculation of the dipolar terms of Hamiltonian 2 are readily expressed in terms of the set of polar coordinates (r, θ, φ) defining the location of m in the frame (X, Y, Z) . The orientation of the magnetic axes (x, y, z) of the $[4\text{Fe}-4\text{S}]^+$ cluster with respect to (X, Y, Z) is specified by the set of Euler angles $(\alpha', \beta', \gamma')$ and the orientation of the magnetic axes of the mononuclear center m with respect to (x, y, z) is defined by the set (α, β, γ) .

To end this section, we present a series of EPR spectra calculated from the local spin model, in the simple case of a $[4\text{Fe}-4\text{S}]^+$ cluster characterized by an isotropic g tensor ($g_x = g_y = g_z = 1.95$) coupled by purely dipolar interactions to a mononuclear center m characterized by $g_m = 2.15$. In order to

illustrate the importance of the position of the mononuclear center with respect to the $[4\text{Fe}-4\text{S}]^+$ cluster, calculations were made with $\varphi = 0$ and $\theta = 0^\circ, 45^\circ, 90^\circ, 135^\circ, 180^\circ$, for two intercenter distances r equal to 10 and 7 Å. We have shown in a previous study that, for a system made of a dinuclear cluster coupled to a mononuclear center or another dinuclear center, the local spin Hamiltonian can be replaced by an equivalent point dipole Hamiltonian when the relative arrangement of the centers is such that all the metal sites of the system are collinear. The effective distance to be used in this equivalent point dipole Hamiltonian is simply expressed in terms of the intersite distances and of the spin coupling coefficients K_i .¹ For a collinear arrangement of the four Fe atoms and of the mononuclear cluster m , the effective distance is given by

$$r_{\text{eff}}^{-3} = K_1 r_{cm}^{-3} + K_2 r_{dm}^{-3} + (r_{am}^{-3} + r_{bm}^{-3})(K_3 + K_4)/2 \quad (8)$$

No such collinear arrangement is of course possible for a system containing a $[4\text{Fe}-4\text{S}]$ cluster. Nevertheless, we have compared the EPR spectra given by the local spin model to those calculated with a point dipole model (program POINTDIP¹) with a distance given by eq 8. The EPR spectra calculated in this way are represented in Figure 2. For a given distance r , we observe that the shape of the spectrum given by the local spin model depends strongly on the θ value defining the orientation of m . When θ is close to 0° or 180° , the main features of the spectrum are approximately reproduced by a point dipole calculation using the r_{eff} value given by eq 8. This property is conserved when φ is different from zero.²¹ It is due to the fact that when the intercenter axis is close to Z , m is almost equidistant from the equivalent sites, a and b on the one hand and c and d on the other hand (Figure 1), so that the dipolar terms of the local spin Hamiltonian almost reduce to that of the point dipole model provided that r is not too small. Thus, although the spectra represented in Figure 2 correspond to the particular case of two isotropic paramagnets, they illustrate a more general behavior and help understanding why the point dipole approximation can give in some cases good simulations of experimental EPR spectra.

Study of the Magnetic Interactions between the Nickel Center and the Proximal $[4\text{Fe}-4\text{S}]^+$ Cluster in *D. gigas* Hydrogenase

Hydrogenases are enzymes involved in the production and consumption of molecular hydrogen by microorganisms. The Ni-Fe hydrogenase from *Desulfovibrio gigas* contains a nickel center which is considered as being the active site and three iron-sulfur centers, two $[4\text{Fe}-4\text{S}]^{2+,1+}$ and one $[3\text{Fe}-4\text{S}]^{1+,0}$ clusters.²² When isolated in aerobic conditions, the enzyme is inactive and requires a prolonged incubation with reductants to recover its catalytic activity. During reduction in the presence of hydrogen, an EPR signal called Ni-C characterized by g values at 2.19, 2.14, and 2.01 is observed.²³ Upon further reduction, the $[4\text{Fe}-4\text{S}]$ clusters become paramagnetic and interact magnetically with the Ni center, giving a complex EPR spectrum called the split Ni-C signal which is only visible at low temperature.^{24,25} A recent X-ray crystal study carried out at 2.85 Å resolution has shown that, in the inactive form of the

(21) Camensuli, P. Thèse de doctorat, Université de Provence, Marseille, 1995.

(22) Hatchikian, E. C.; Fernandez, V. M.; Cammack, R. *FEMS Symp.* **1990**, *54*, 53-73.

(23) Fernandez, V. M.; Hatchikian, E. C.; Patil, D.; Cammack, R. *Biochim. Biophys. Acta* **1986**, *883*, 69-79.

(24) Cammack, R.; Patil, D.; Hatchikian, E. C.; Fernandez, V. M. *Biochim. Biophys. Acta* **1987**, *912*, 98-109.

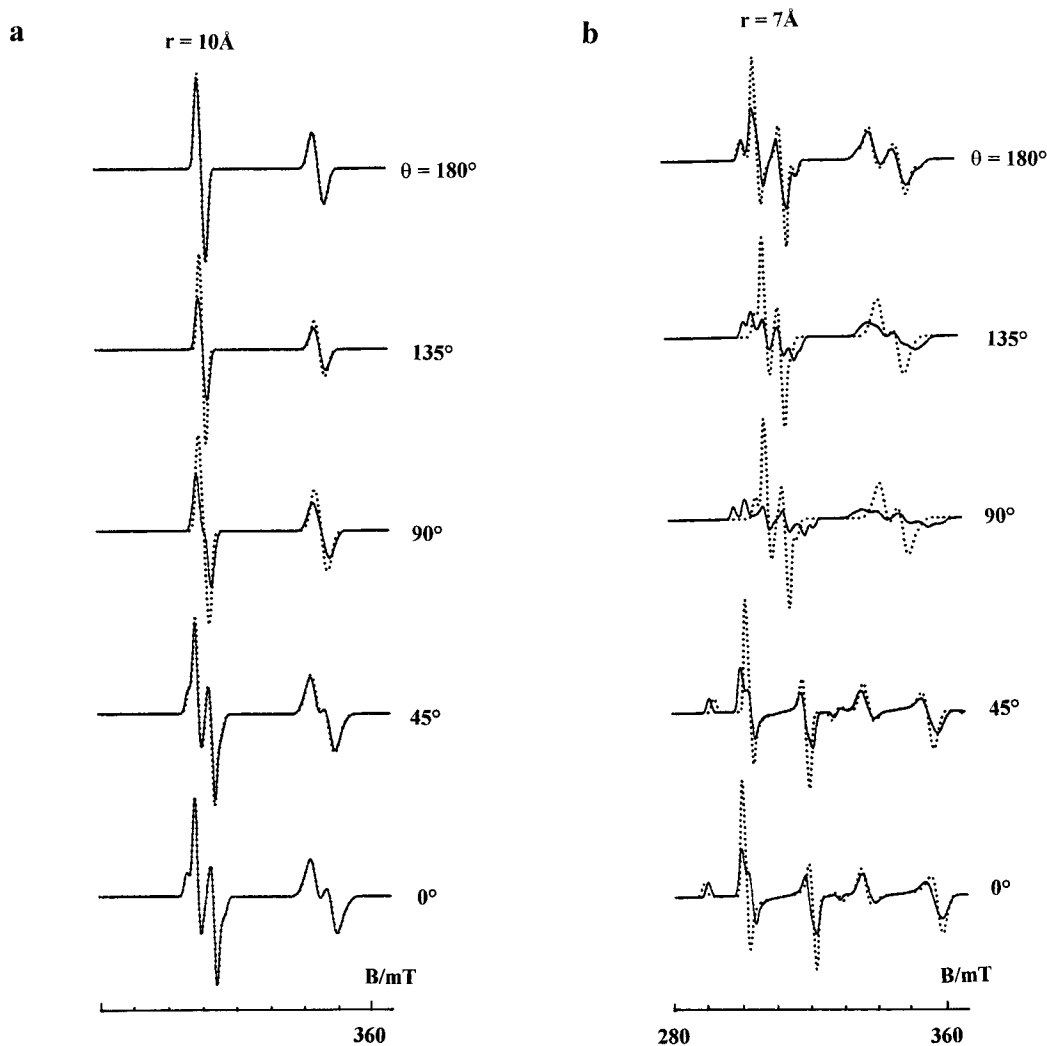


Figure 2. Comparison of EPR spectra calculated from the point dipole and local spin models for a system made of a $[4\text{Fe}-4\text{S}]^+$ cluster characterized by an isotropic g tensor ($g_x = g_y = g_z = 1.95$) coupled by dipolar interactions to a mononuclear center m characterized by $g_m = 2.15$. r is the intercenter distance, θ is the angle ($\hat{Z}, \text{O}\hat{m}$). Solid lines: spectra computed from the local spin Hamiltonian 2; dotted lines: spectra computed from the point dipole Hamiltonian with the value r_{eff} given by eq 8. For a given set (r, θ), the spectra are normalized in intensity. The microwave frequency used in the calculations was 9.300 GHz. The peak-to-peak line width of the $[4\text{Fe}-4\text{S}]^+$ and mononuclear centers were taken equal to 2.6 and 1.6 mT, respectively.

enzyme, the four metal centers are organized according to a quasi linear arrangement in which the first neighbor of the Ni center is a $[4\text{Fe}-4\text{S}]$ cluster called “proximal” by the authors.⁶ In a previous work, we have begun to investigate this arrangement in the active form of the enzyme, by studying the intercenter magnetic interactions responsible for the split Ni–C signal.⁵ We showed in particular that good simulations of this signal could be obtained by the point dipole model by assuming that it arises from the coupling of the Ni center with a single $[4\text{Fe}-4\text{S}]^+$ cluster, in agreement with the results of the crystal study (Figure 3a–c).

Since this study was based on the point dipole model, it could not bring detailed information on the relative arrangement of the two centers. In order to compare this arrangement in the active and inactive forms of the enzyme, it is necessary to resort to the local spin model described in the previous section. Some of the parameters involved in this model are identical to or are expected to be similar to those given by our previous work. Among these parameters are, of course, the g values and line width parameters of the Ni center, which were determined

through a numerical simulation of the unsplit Ni–C signal.⁵ In addition, the exchange interactions are treated in the same way in the point dipole and in the local spin description (Hamiltonian 2), so that the values of the parameter J and of the Euler angles (α, β, γ) defining the relative orientation of the Ni center magnetic axes with respect to those of the $[4\text{Fe}-4\text{S}]^+$ cluster are expected to be similar in both models.

Actually, the two models differ essentially by their treatment of the dipolar interactions. In our previous work, good simulations were obtained from the point dipole model by using an effective distance equal to 8.6 Å,⁵ a value much smaller than the intercenter distance of about 12 Å given by the X-ray crystal study. We have seen in the preceding section that the main features of EPR spectra calculated with the local spin model are approximately reproduced by the point dipole model provided that the effective distance r_{eff} defined by eq 8 is used. The distance of 8.6 Å given by our previous study then contains useful information about the orientation of the Ni center with respect to the $[4\text{Fe}-4\text{S}]^+$ cluster. We have represented in Figure 4 the variations of r_{eff} given by eq 8 as a function of the polar angles (θ, φ) defining the Ni center direction (Figure 1) for $r = 12$ Å. When θ is small, r_{eff} is weakly dependent on φ and is significantly smaller than the intercenter distance r . For θ values

(25) Teixeira, M.; Moura, I.; Xavier, A. V.; Moura, J. J.; LeGall, J.; Dervartanian, D. V.; Peck, H. D.; Huynh, B. H. *J. Biol. Chem.* **1989**, *264*, 16435–16450.

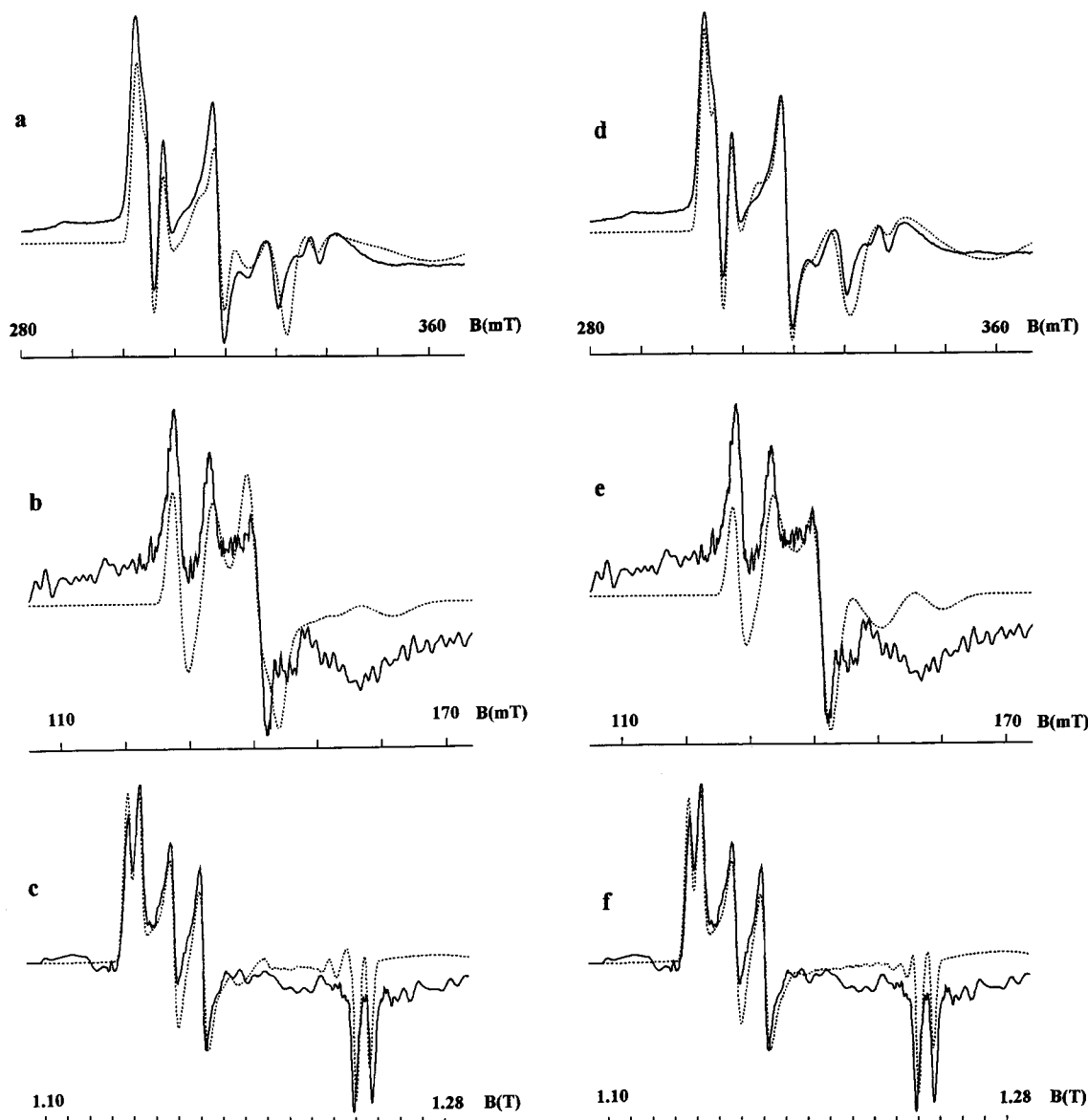


Figure 3. Numerical simulation of the split Ni–C signal of *D. gigas* hydrogenase recorded at X-band, S-band, and Q-band. Solid lines, experimental spectra recorded at the following frequencies: (a,d), 9.378 GHz; (b,e), 4.051 GHz; and (c,f), 34.95 GHz. Other conditions as in Figure 3 of ref 5. Dotted lines: simulations obtained with the point dipole model (a,b,c), the local spin model (d,e,f), and the parameters listed in Table 1.

exceeding 90° , r_{eff} depends strongly on φ and is larger than r . Magic magnetic configurations for which the dipolar terms cancel occur for particular values of (θ, φ) (Figure 4). Similar variations of r_{eff} are observed when r varies in the range 10–14 Å. In view of these variations, the distance of 8.6 Å given by the point dipole model indicates that the angle θ defining the orientation of the Ni center with respect to the $[4\text{Fe}-4\text{S}]^+$ cluster is small in *D. gigas* hydrogenase, which means that the Ni center is on the side of the mixed-valence pair of the $[4\text{Fe}-4\text{S}]^+$ cluster (Figure 1).

These different pieces of information restricted considerably the relevant part of the parameters' space, which could then be systematically explored by resorting to the program REGRES described in Materials and Methods. The adjustable parameters were determined so as to produce the best simulations at X-band, S-band, and Q-band. As expected, the strongest constraints arose from the X-band and S-band spectra. The best simulations obtained in this way are represented in Figure 3d–f, and the corresponding set of magnetic and structural parameters are reported in Table 1. Owing to the number of adjustable parameters, it is difficult to give an error interval for each of them. However, it is worth noting that acceptable although

lesser quality simulations were obtained by using slightly different arrangements, provided that the set (θ, φ) remains close to $(54^\circ, 45^\circ)$, which corresponds to a cube diagonal going through one of the mixed-valence Fe ions (Figure 1), and that the intercenter distance r remains in the range 11.4–11.9 Å. In order to illustrate the sensitivity of the simulations with respect to the relative arrangement of the interacting centers, we have represented in Figure 5 the best simulations obtained at X-band and S-band for other orientations of the intercenter axis in the plane defined by the axis Z and the mixed-valence pair (a,b) (Figure 1). For $\theta = 0^\circ$ and 90° , the quality of the S-band simulations (Figure 5b,d) is almost as good as that of Figure 3e, but the position and the relative amplitude of the main features of the X-band spectra are not well reproduced (Figure 5a,c). For $\theta = 180^\circ$, acceptable S-band spectra can only be obtained at the expense of very bad X-band simulations (Figure 5e,f).

In order to completely validate the data reported in Table 1, it is important to test the sensitivity of the calculated spectra with respect to some basic assumptions made in the treatment of eqs 5 giving the local magnetic moments involved in the calculation of the dipolar terms of Hamiltonian 2. A first

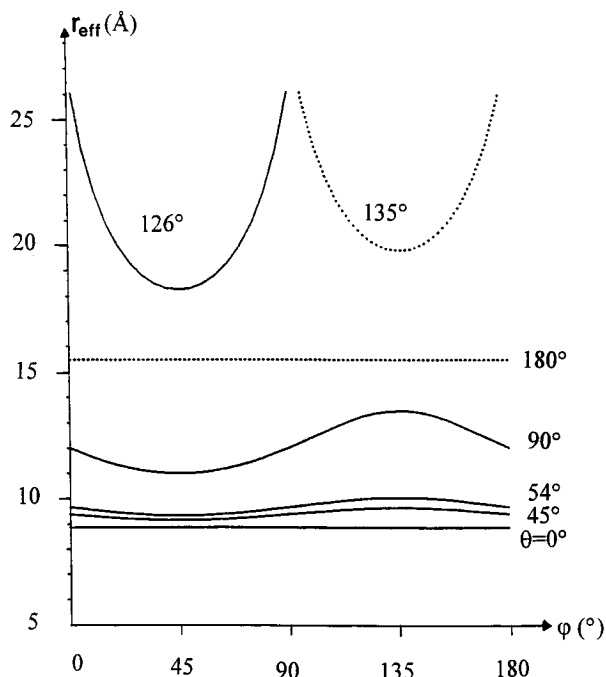


Figure 4. Variations of the effective distance r_{eff} given by eq 8 as a function of the polar angles (θ , φ) defining the direction of the Ni center for $r = 12 \text{ \AA}$. r_{eff} can be positive (solid lines) or negative (dotted lines).

Table 1. Parameters Values Used in the Best Simulations of the Split Ni–C EPR Signal of *D. gigas* Hydrogenase

parameter	local spin model	point dipole model
FeS center ^a		
g_x, g_y, g_z	1.880, 1.910, 2.145	1.860, 1.915, 2.137
$\sigma_x, \sigma_y, \sigma_z$	$30 \times 10^{-3}, 30 \times 10^{-3}, 40 \times 10^{-3}$	$30 \times 10^{-3}, 30 \times 10^{-3}, 40 \times 10^{-3}$
$J (\text{cm}^{-1})$	41×10^{-4}	40×10^{-4}
α, β, γ^b	45°, 63°, 109°	56°, 72°, 105°
r, θ, φ	11.7 Å, 61°, 69° ^c 11.7 Å, 48°, 48° ^d	8.6 Å, 86°, 60° ^c
$\alpha', \beta', \gamma'^e$	95°, 95°, -15°	

^a The g values and line width parameters of the Ni center are identical to those given in Table 1 of ref 5. ^b Euler angles defining the orientation of the magnetic axes of the Ni center with respect to those of the $[4\text{Fe}-4\text{S}]^+$ cluster. ^c Polar coordinates defined with respect to the magnetic axes (x, y, z) of the $[4\text{Fe}-4\text{S}]^+$ cluster. ^d Polar coordinates defined with respect to the (X, Y, Z) axes system of the $[4\text{Fe}-4\text{S}]^+$ cluster (Figure 1). ^e Euler angles defining the orientation of the magnetic axes of the $[4\text{Fe}-4\text{S}]^+$ cluster with respect to the set (X, Y, Z).

assumption concerns the values of the spin coupling coefficients K_i , which depend on the spin coupling scheme chosen for the $S = 1/2$ ground state of the $[4\text{Fe}-4\text{S}]^+$ cluster. The simulations presented in Figure 3d–f were carried out by using the set of K_i given by eq 6. We found that equivalent simulations could be obtained by using very similar structural parameters and the set $K_1 = K_2 = -1$, $K_3 = 37/21$, $K_4 = 26/21$ corresponding to a $S = 1/2$ ground state arising from the coupling between $S_{12} = 3$ and $S_{34} = 7/2$.^{12,13} Thus, the difference between these two sets of K_i is not sufficient to permit our model to discriminate between the two spin coupling schemes.

In the previous section, we have shown that several arguments favor a fully delocalized mixed-valence pair for the $S = 1/2$ ground state of $[4\text{Fe}-4\text{S}]^+$ clusters. However, as suggested by the reviewers, it is interesting to examine whether the calculated spectra represented in Figure 3d–f are sensitive to the level of electron delocalization of this pair. For a given geometrical arrangement of the interacting center defined in Figure 1, the two extreme situations with regard to electron

delocalization correspond to the localization of the excess electron on site a or on site b. According to eq 5, the magnetic moments are given in the first case by $\vec{\mu}_a = -\beta K_4 \tilde{g}_4 \vec{S}$, $\vec{\mu}_b = -\beta K_3 \tilde{g}_3 \vec{S}$, and in the second case by permuted expressions. In the procedure used in the calculation of the dipolar terms, \tilde{g}_3 and \tilde{g}_4 are replaced by isotropic values g_3 and g_4 which are related through eq 7. In the case of the $[4\text{Fe}-4\text{S}]^+$ cluster of *D. gigas* hydrogenase, this leads to $g_3 = 2.025$ and $g_4 = 2.07$, so that $K_4 g_4$ and $K_3 g_3$ are equal to 3.37 and 4.12, respectively. These numbers do not differ much, so that the spectra calculated by localizing the excess electron on site a or b are expected to be very similar. This was borne out by comparing spectra calculated for these two localizations with the parameters reported in Table 1, for different values of the set (θ, φ) which defines the location of the Ni center with respect to the $[4\text{Fe}-4\text{S}]^+$ cluster (Figure 1). Whatever the relative arrangement of the two centers, permuting $\vec{\mu}_a$ and $\vec{\mu}_b$ produced no or very little change on the EPR spectrum. From this study, it can be concluded that the calculated spectra are essentially insensitive to the level of valence delocalization within the mixed-valence pair of the $[4\text{Fe}-4\text{S}]^+$ cluster. Since this result is related to the closeness of K_3 and K_4 , it could be general in the case of $[4\text{Fe}-4\text{S}]^+$ clusters characterized by a $S = 1/2$ ground state.

Discussion

We have recalled in Figure 3 the best simulations given by the point dipole model, which were obtained with the set of parameters reported in Table 1. Comparing the spectra of Figure 3 shows that the medium and high field part of the X-band spectrum and the relative amplitudes of the different peaks of the S-band spectrum are much better reproduced by the local spin model. Indeed, at X-band, the parameter χ^2 defined in Materials and Methods is equal to 7.4×10^{-2} and 2.9×10^{-2} for the simulations represented in Figure 3a,d, respectively. The residual difference between the experimental spectra and those calculated with the local spin model may have two different origins (i) in our calculations, the line width of the spectra is assumed to originate only from g -strain effects, whereas previous simulations have shown that J - r strain can be a source of appreciable broadening^{1,26} (ii) more importantly, it should be realized that the experimental spectrum does not result solely from the magnetic interactions between the Ni center and the proximal $[4\text{Fe}-4\text{S}]^+$ cluster. First, the redox state of the sample is such that part of the spectrum arises from fully reduced hydrogenase molecules in which the Ni center is not paramagnetic. In these molecules, the proximal $[4\text{Fe}-4\text{S}]^+$ cluster gives a broad EPR signal which is clearly visible at $g_x = 1.88$ on the high field part of the experimental S-band spectrum (Figure 3e). Secondly, the distal $[4\text{Fe}-4\text{S}]^+$ cluster which is not magnetically coupled to the Ni center also contributes to the Fe–S signal. Finally, the presence of a nearby paramagnetic $[3\text{Fe}-4\text{S}]^0$ cluster may also modify the lineshape of the $[4\text{Fe}-4\text{S}]^+$ signals. All these effects contribute to the baseline of the split Ni–C signal. We have not attempted to take these complex effects into account. However, we have observed that the quality of the fit could be significantly improved by attributing anomalously large line widths to the proximal $[4\text{Fe}-4\text{S}]^+$ cluster in order to model roughly the broad Fe–S signal.²¹

It is interesting to compare the values of the parameters given by the point dipole and local spin models (Table 1). We first observe that the exchange parameter J and the Euler angles (α, β, γ) defining the relative orientation of the magnetic axes of the Ni center and of the $[4\text{Fe}-4\text{S}]^+$ cluster are very similar in both models, as anticipated in the previous section. This is due to the fact that the effect of the exchange interactions, which

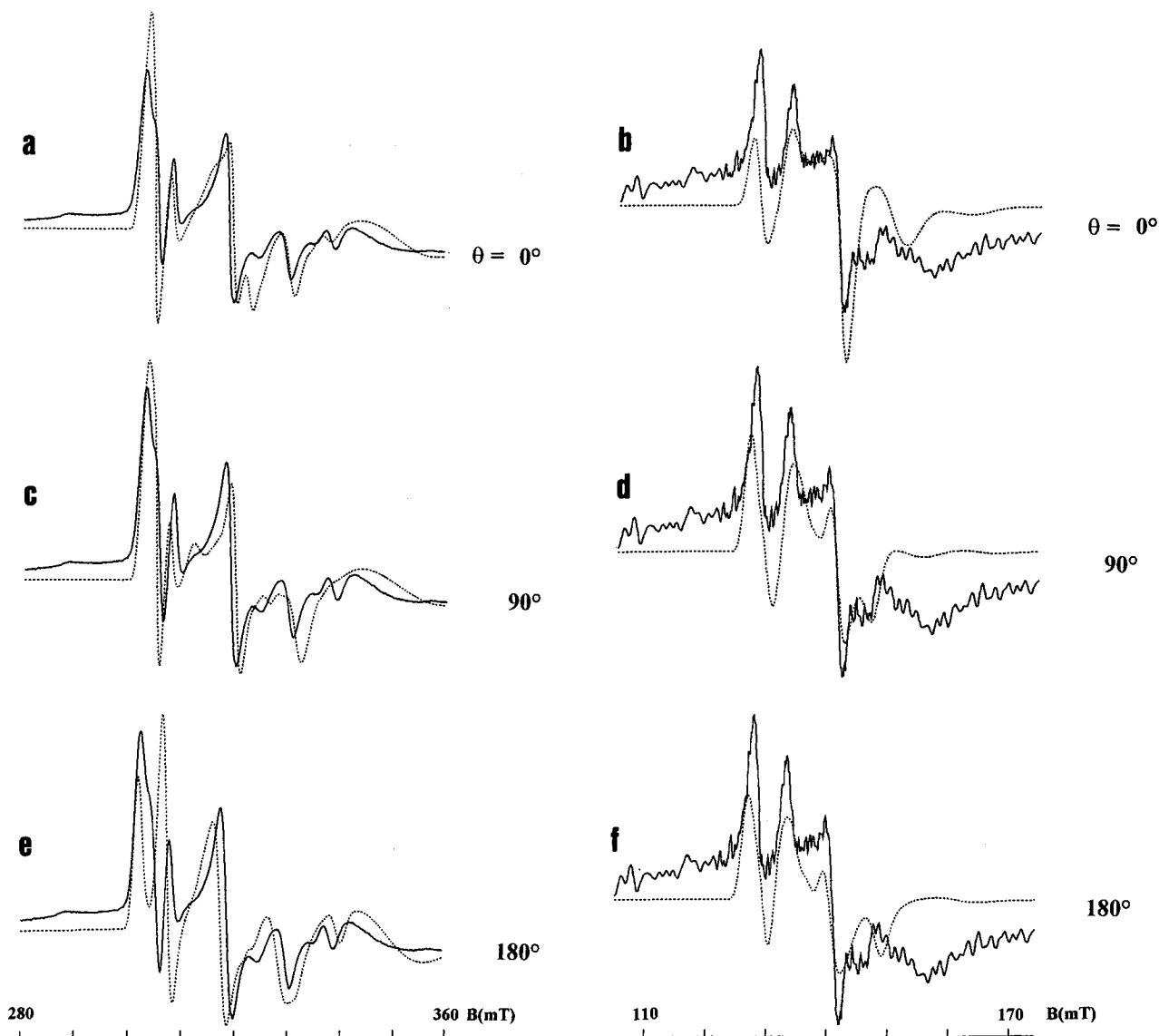


Figure 5. Simulation of the X-band and S-band split Ni-C EPR spectra given by the local spin model for different orientations of the Ni center in the plane defined by the axis Z and the mixed-valence pair (a,b) of the $[4\text{Fe}-4\text{S}]^+$ cluster ($\varphi = 45^\circ$, see Figure 1). The best simulations (dotted lines) at X-band (a,c,e) and S-band (b,d,f) were obtained with the following sets of parameters: (a) and (b) $\theta = 0^\circ$, $r = 11.1 \text{ \AA}$, $J = 41 \times 10^{-4} \text{ cm}^{-1}$, $\alpha = 15^\circ$, $\beta = 98^\circ$, $\gamma = 123^\circ$, $\alpha' = 90^\circ$, $\beta' = 45^\circ$, $\gamma' = 90^\circ$; (c) and (d) $\theta = 90^\circ$, $r = 9.7 \text{ \AA}$, $J = 42 \times 10^{-4} \text{ cm}^{-1}$, $\alpha = -5^\circ$, $\beta = 57^\circ$, $\gamma = 64^\circ$, $\alpha' = 0^\circ$, $\beta' = 90^\circ$, $\gamma' = 0$; (e) and (f) $\theta = 180^\circ$, $r = 8 \text{ \AA}$, $J = 41 \times 10^{-4} \text{ cm}^{-1}$, $\alpha = 45^\circ$, $\beta = 63^\circ$, $\gamma = 70^\circ$, $\alpha' = 95^\circ$, $\beta' = 95^\circ$, $\gamma' = -15^\circ$. Other parameters are as in Table 1.

determines to a great extent the position of the main features of the split Ni-C spectrum, depends strongly on this relative orientation and on the J value.⁵ Next, we consider the direction of the intercenter axis with respect to the $[4\text{Fe}-4\text{S}]^+$ magnetic axes. In the point dipole model, the effect of the dipolar interactions depends only on the orientation of the intercenter vector \vec{r} with respect to the magnetic axes, whereas in the local spin description it also depends on the orientation of \vec{r} with respect to the $[4\text{Fe}-4\text{S}]^+$ cubane structure. Therefore, the polar angles (θ, φ) given by the two models are expected to be different. Nevertheless, the values reported in Table 1 are quite similar, so that the angle between the two directions is calculated to be only 25° . This confirms an earlier observation made in our previous studies of photosystem I and xanthine oxidase, concerning the relevance of the angular parameters given by simulations based on the point dipole model.^{1,26}

We now consider the parameters specific to the local spin model. The values of the Euler angles (α', β', δ') defining the

orientation of the magnetic axes of the $[4\text{Fe}-4\text{S}]^+$ cluster with respect to the system (X, Y, Z) represented in Figure 1 are such that the magnetic axes are nearly perpendicular to the faces of the 4Fe cube (Table 1). Such an orientation has already been observed for $[4\text{Fe}-4\text{S}]^+$ synthetic analogues.¹⁸⁻²⁰ However, in our case the magnetic axis which is nearly perpendicular to both the ferrous (Fe(II), Fe(II)) pair and the mixed-valence (Fe(III), Fe(II)) pair corresponds to the intermediate g_y component, whereas it has been proposed to correspond to the largest g_z component in the case of the synthetic analogues.²⁰ We have checked that no acceptable simulation could be obtained by using this last attribution. Although other studies are needed before this result is fully interpreted, it is tempting to speculate that the peculiar orientation found for the proximal $[4\text{Fe}-4\text{S}]^+$ center of *D. gigas* hydrogenase could be related to the very anisotropic g tensor found for this cluster (Table 1).

According to the X-ray crystal structure carried out on the inactive form of *D. gigas* hydrogenase, the proximal $[4\text{Fe}-4\text{S}]$ cluster is bound to a N-terminal domain which is highly conserved in Ni-containing hydrogenases, suggesting that this

(26) Guigliarelli, B.; Guillaussier, J.; More, C.; Setif, P.; Bottin, H.; Bertrand, P. *J. Biol. Chem.* **1993**, *268*, 900-908.

cluster plays an important role in the enzymatic mechanism.⁶ It is then especially interesting to compare the relative arrangement of this cluster and of the Ni center in the active form of the enzyme to that given by the crystal study. The values of the center-to-center distance r given by the two studies are 11.7 Å (Table 1) and 12.3 Å (Volbeda, A.; Frey, M.; Fontecilla, J., personal communication), respectively, and agree probably within experimental errors. In our study, the orientation of the intercenter axis with respect to the (X,Y,Z) system represented in Figure 1 is defined by the polar angles $\theta = 48^\circ$, $\varphi = 48^\circ$, which are very close to the values $\theta = 54^\circ$, $\varphi = 45^\circ$ corresponding to the cube diagonal going through one iron atom, say b, of the mixed-valence pair. Indeed, it can be calculated that the angle O–b–Ni is equal to 170° , where O is the center of the cube. This arrangement is very similar to that arrived at by the X-ray crystal study, according to which the Ni atom almost lies on the cube diagonal going through iron atom Fe₁ ligated to Cys17S, the angle O–Fe₁–Ni being equal to 174° (Volbeda, A.; Frey, M.; Fontecilla, J., personal communication). From this comparison, it can be concluded that the conformational changes that occur upon the activation process do not modify appreciably the relative arrangement of the Ni center and of the proximal [4Fe–4S] cluster. Furthermore, our study permits us to assess that Fe₁ coordinated to Cys17S is one of the mixed-valence irons of the reduced [4Fe–4S]⁺ cluster. Unfortunately, the fact that the three other iron atoms of the cluster are nearly related one to another by a threefold rotation around the intercenter axis precludes the attribution of the second mixed-valence iron.

So far, we have represented the Ni center by a point dipole, which is certainly a very good approximation if this center is mononuclear. However, the X-ray study has revealed the existence of a metal X located at about 2.9 Å from the Ni ion,⁶ so that the possibility of a spin coupled dinuclear active site must be envisaged. In fact, several experimental data argue for the Ni center being an uncoupled Ni–X center. First, the g values and ⁶¹Ni hyperfine constants observed on the Ni–C signal of *D. gigas* hydrogenase are very similar to those measured for oxidized nickel-substituted rubredoxin, which contains a Ni(III) center coordinated by four cysteine residues.²⁷ Secondly, recent experiments carried out in our laboratory have demonstrated that the temperature dependence of the Ni–C signal is typical of a magnetically isolated $S = 1/2$ mononuclear center (Dole, F.; Guigliarelli, B., unpublished results). Lastly, if the (Ni–X) center were a spin coupled dinuclear cluster, it should be described according to the local spin model presented

(27) Huang, Y. H.; Park, J. B.; Adams, M. W. W.; Johnson, M. K. *Inorg. Chem.* **1993**, *32*, 375–376.

in ref 1 for the calculation of the split Ni–C EPR spectrum. This would probably change the values of the structural parameters deduced from the numerical simulation. Owing to the very good agreement between the arrangements of the Ni center and of the [4Fe–4S]⁺ cluster given respectively by the crystal study and by the present work, the hypothesis of an uncoupled (Ni–X) center appears as the most likely.

Conclusion

In this paper, we have developed a local spin model to describe the magnetic interactions between a [4Fe–4S]⁺ cluster and a mononuclear center, which takes into account the electron delocalization within the mixed-valence (Fe(III),Fe(II)) pair. This model can be easily extended to other iron–sulfur centers containing mixed-valence pairs, like [3Fe–4S]⁰ and [4Fe–4S]³⁺ clusters. Although including delocalization effects results in a significant increase of the number of unknown parameters in the model, the interaction spectrum is expected to be weakly sensitive to several of them. For example, in the present work, nearly identical spectra were obtained by using isotropic or anisotropic ferrous g tensors in the calculation of the dipolar terms and by using two different sets of spin coupling coefficient K_i . Likewise, the spectra were found almost insensitive to the level of electron delocalization within the mixed-valence pair. Therefore, our study provides no information about the orientation of the local g tensors, about the spin coupling scheme leading to the $S = 1/2$ ground state, and about the level of valence delocalization within the (Fe(III), Fe(II)) mixed-valence pair of the [4Fe–4S]¹⁺ cluster. Conversely, the parameters describing the relative arrangement of the two centers could be determined accurately without resorting to any peculiar assumption concerning these different points. These properties are certainly not restricted to the case of *D. gigas* hydrogenase, and they will be systematically studied in our future investigations.

The results obtained in this work and in our previous study on *D. gigas* hydrogenase⁵ bring a piece of information which is quite important on the methodological point of view. Comparing the magnetic and structural parameters given by the local spin model to those obtained by the point dipole model confirms our earlier observations concerning the validity of the angular parameters deduced from numerical simulations based on the point dipole model. Thus, although only the local spin model is able to provide a detailed description of the relative arrangement of the two interacting centers, numerical simulations based on the point dipole model constitute a very useful first step.

JA951981W